ROYAL SOCIETY
OF CHEMISTRY

## PAPER

Check for updates

# A modeling framework to identify environmentally greener and lower-cost pathways of nanomaterials†

Kai Lan,[a,b] Hannah Szu-Han Wang,[a] Tessa Lee,[a] Camilla Abbati de Assis,[c] Richard A. Venditti, [b] Yong Zhu[d] and Yuan Yao [*a,e]

Producing environmentally benign and economically viable nanomaterials is critical for large-scale applications in energy and other industries. This study presents a modeling framework to identify environmentally greener and lower-cost pathways of large-scale nanomaterial production, which encompasses life cycle assessment, Green Chemistry principles, techno-economic analysis, and eco-efficiency analysis. The framework is demonstrated by case studies of cellulose nanomaterials produced in the U.S. For cellulose nanocrystals, the framework identifies pathways that simultaneously reduce the life-cycle global warming potential (GWP) from 17.7 to 2.6 kgCO₂e per dry kg cellulose nanocrystals and the minimum selling price (MSP) from US$7540 to US$4587 per dry t cellulose nanocrystals. For cellulose nanofibrils, the strategies present trade-offs of reducing GWP from 7.8 to 0.1 kgCO₂e per dry kg cellulose nanofibrils but increasing MSP slightly from US$2873 to US$2985 per dry t cellulose nanofibrils. Eco-efficiency analysis quantifies the magnitudes of co-benefits and trade-offs between the environmental and economic performance of different production strategies and supports decision making for sustainability-informed process optimization.

## 1. Introduction

The unique properties and performance of nanomaterials have attracted much attention in various fields, such as energy, electronics, water treatment, medicine, and agriculture.[1–3] Sustainable design and development of nanomaterials need holistic consideration of environmental sustainability, economic viability, and material functionality.[4] Metrics-based frameworks have been developed, such as the well-known Ashby material selection framework and other adapted frameworks that include more environmental and human health considerations.[2,4,5] These frameworks focus on streamlined nanomaterial screening and selection, which suit early-stage material design; however, more comprehensive assessments are needed to understand potential environmental impacts

and techno-economic performance for large-scale commercial production and application of nanomaterials.[6] Life cycle assessment (LCA) and techno-economic analysis (TEA) have been explored for specific nanomaterial classes and applications.[6–9] Previous studies have shown large variations in the environmental and economic performances of different nanomaterial production pathways; however, it is unclear how the pathways of reducing environmental burdens affect the economic feasibility of nanomaterial production. There is a strong need to understand the drivers of and trade-offs/co-benefits between the economic and environmental performance of different nanomaterials production pathways and provide guidance on how to use such understandings to inform process design and optimization for producing greener and more cost-effective nanomaterials.

To address this gap, we develop a framework powered by LCA, Green Chemistry (GC) principles, TEA, and eco-efficiency analysis to identify the pathways of producing greener and lower-cost nanomaterials. In this framework, LCA assesses the life-cycle environmental impacts of a material;[10–12] TEA evaluates the economic performance of emerging technologies and various production pathways.[6,13,14] This framework uses the GC principles to develop improvement strategies and scenarios towards greener production.[15–18] An eco-efficiency analysis quantifies the co-performance of a product in environmental and economic dimensions; eco-efficiency is typically measured as the ratio of environmental impacts to economic value or

*[a]Center for Industrial Ecology, Yale School of the Environment, Yale University, 380 Edwards Street, New Haven, Connecticut, 06511, USA. E-mail: y.yao@yale.edu*
*[b]Department of Forest Biomaterials, North Carolina State University, 2820 Faucette Drive, Raleigh, North Carolina, 27695, USA*
*[c]Fisher International, Inc., 15720 Brixham Hill Ave. Suite 550, Charlotte, North Carolina, 28277, USA*
*[d]Department of Mechanical and Aerospace Engineering, North Carolina State University, 911 Oval Drive, Raleigh, North Carolina, 27695, USA*
*[e]Chemical and Environmental Engineering, Yale School of Engineering and Applied Science, Yale University, 17 Hillhouse Avenue, New Haven, Connecticut, 06520, USA*
†Electronic supplementary information (ESI) available. See DOI: https://doi.org/10.1039/d3gc04036d

*vice versa.*[19,20] We demonstrate this framework through a conceptual case study of cellulose nanomaterials in the U.S. at a large scale.

Cellulose nanomaterials have received increasing research interest due to their high mechanical strength, aspect ratio, biodegradability, biocompatibility, and other advantages.[21] Two common categories of cellulose nanomaterials are cellulose nanofibrils (CNF) and cellulose nanocrystals (CNC).[22] CNC are "rod-like" or "needle-like" nanoparticles with high crystallinity, while CNF may have higher amorphous cellulose than CNC and a larger aspect ratio (length/width).[23] Besides the morphological differences, CNC- and CNF-based materials can differ in mechanical properties (*e.g.*, tensile strength and density).[23–27] Many applications of cellulose nanomaterials have been reported, *e.g.*, coatings,[28] gel inks,[29] tissue engineering,[30] wound dressing,[31] smart sensors,[32] and soft electronics.[33] Previous LCA has shown high environmental burdens of CNC and CNF, majorly due to high energy consumption, waste produced, and chemical usage (*e.g.*, acid, neutralizing agent).[34] Hence, exploring the pathways of reducing environmental burdens and production cost is essential for large-scale commercial production of CNC and CNF.[34] Previous LCA and TEA studies have investigated the environmental impacts and economic feasibility of CNC or CNF production with different methods (see ESI Section S1 for literature review†).[21,34–49] However, few studies have explored varied process design strategies (*e.g.*, different choices of acid recovery, energy sources, and neutralizing agents) or alternative production means (*e.g.*, organic or inorganic acid,[21,39] acid hydrolysis or autohydrolysis,[38,50] with or without pretreatment[35,38]). Nor have they simultaneously explored the corresponding economic performance of alternative pathways and the potential trade-offs between the environment and economic performance. Additionally, few studies have considered the end-of-life emissions of CNC and CNF, which is a common challenge for nanomaterial LCAs.[51]

Using this framework, we have identified 11 scenarios (7 scenarios for CNC and 4 scenarios for CNF) to explore their impacts on environmental performance and economic feasibility. The results of production economics and environmental impacts, and their trade-offs/co-benefits provide information for stakeholders (*e.g.*, investors and researchers) on different manufacturing strategies and highlight future opportunities and research directions for producing greener and more cost-effective cellulose nanomaterials. Although the case studies only include CNC and CNF materials, the framework is broadly applicable to other materials and can be applied to other nanomaterials for identifying lower-cost and greener manufacturing pathways.

# 2. Methods and materials

## 2.1. Framework overview

Fig. 1 shows the four main modules of the framework: pathway selection and process analysis, LCA, TEA, and result interpretation. Pathway selection starts from a baseline scenario that can be current practices or traditional/emerging technologies that have not been optimized. Then alternative pathway scenarios (Scenario $j_1, j_2, ..., j_k$) are generated by applying relevant GC principles. One or multiple changes can be added in one scenario, depending on the expected granularity in understanding the effects of changes. If an alternative pathway (Scenario $j_k$) has met improvement criteria compared to the previous scenario (Scenario $j_{k-n}$, $n$ depends on technology choices), then the scenario is selected for further improvement. Otherwise, the scenario is rejected. These improvement criteria can be lowered environmental impacts, better economic performance, or improved material circularity, depending on the users' needs. This study only focuses on carbon and economic improvement as a demonstration, but other focuses, such as circular economy principles[52,53] can be easily incorporated. Future users can also set rejection criteria (*e.g.*, at least 5% poorer performance). Process analysis for each scenario provides mass and energy balances that are essential inventory data needed by LCA. Various methods can be used for process analysis, including theoretical calculations, process simulation, data-driven approach, and other methods.[54] This study adapts the TEA framework proposed by Zimmermann *et al.*[55] The selection of specific environmental and economic indicators depends on the goal and purpose of projects and will need to be determined on a case-by-case basis. The results of LCA and TEA can be interpreted separately or incorporated into an eco-efficiency analysis to quantify the extent to which a trade-off or co-benefit exists (see Section 2.8).

## 2.2. Case study overview

The framework is applied to cellulose nanomaterials. 7 scenarios for CNC production and 4 scenarios for CNF production were generated using GC principles (see Sections 2.3 and 2.4, and ESI Sections S2 and S3†). Fig. 2 shows the summarized flow diagram of each scenario (the detailed flow diagrams are shown in ESI Fig. S1–S7†). In this study, the potential improvement pathways were identified from the previous literature that tested the technical feasibility or conducted related experiments. Note that these pathways do not cover all possible opportunities. But future users like researchers and engineers can utilize this framework to analyze the environmental and economic performance of other opportunities or other GC principles and the potential trade-offs or co-benefits.

The mass and energy balances in each scenario were generated by process simulations for each scenario in Microsoft Excel (see results in ESI Section S4, Tables S1 and S2†). In this study, global warming potential (GWP) is selected as the environmental impact indicator to determine the acceptance or rejection of Scenario $j_k$. For eco-efficiency analysis, we adopt the indicator, environmental cost efficiency (ECE), proposed by Hellweg *et al.*[19] to quantify the trade-offs between the environmental and economic performance of various pathways. In this study, the primary functional unit is mass-based as 1 dry kg of cellulose nanomaterials produced; then the results are converted to the performance-based functional unit
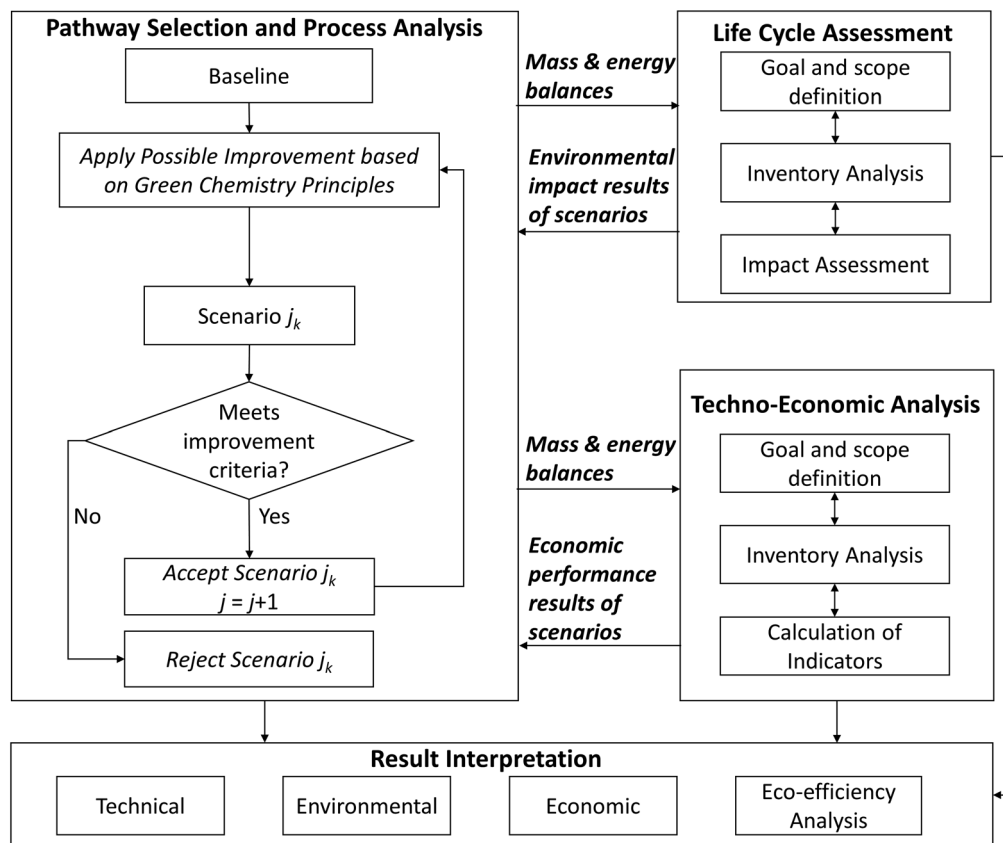
**Fig. 1** Schematic diagram of the modeling framework. The framework consists of four modules, namely pathway selection and process analysis, life cycle assessment, techno-economic analysis, and result interpretation.

that considers material performance (see Section 2.6 for details).

### 2.3. Cellulose nanocrystal production

In this study, the feedstock for CNC production is dissolving pulp which has been widely selected by the previous studies.[38,47,56,57] Dissolving pulp can be produced from varied biomass sources (typically hardwood, softwood, and cotton fibers) *via* sulfite pulping or pre-hydrolysis kraft pulping.[58] In this study, the dissolving pulp type is pre-hydrolysis kraft pulp which is aligned with the pilot plant experiment of Gu *et al.*[38] The compositions of the dissolving pulp are 97.9% (*dry basis*) cellulose, 1.5% xylan (*dry basis*), 0.6% lignin (*dry basis*), with 5.3% moisture content (*dry basis*).[58,59]

For CNC production, there are a total of seven scenarios as mentioned above (all the technical and modeling details are available in ESI Sections S2 and S5†). In the CNC baseline process, the dissolving pulp is first fed into a shredder to generate small particles that allow for sulfuric acid hydrolysis.[38,47,60] After the acid hydrolysis, the hydrolysate is transferred to the tank for dilution with reverse osmosis water and added with sodium chlorite to preserve the brightness.[47] After this step, the acid solution is neutralized by adding 10% NaOH solution.[38] The suspension goes through filtration to remove the remaining large particles. Then the stream is fed

to the diafiltration process for 36 hours to remove sugars and salts and concentrated by the ultrafiltration system to 8 wt%.[38] In the CNC baseline, the unrecovered weak sulfuric acid solution needs to be neutralized with NaOH to generate an effluent consisting of $Na_2SO_4$ and water. Hence, one possible improvement to prevent waste generation can be using CaO to produce gypsum as a byproduct in Scenario CNC-1. After the neutralization, the solids and liquid are separated in the decanter and then gypsum is assumed to be sold. To further prevent waste, Scenario CNC-2 recovers the acid. The acid recovery includes two steps, namely separating $H_2SO_4$ from the hydrolysate and then concentrating the acid solution to 64 wt%.[47] The separation step uses electrodialysis with 90% recovery efficiency.[61,62] Then, the separated sulfuric acid solution is evaporated in a three-effect evaporator to achieve 64 wt% and sent back to the acid hydrolysis reactor.

Solvent selection is one of the most important research areas in GC. Many conventional solvents have issues related to toxicity or corrosion.[15] Energy-intensive distillation for solvent recovery is another concern.[15] To improve the environmental performance of CNC production based on this principle, two possible alternative solvents have been identified in the previous literature: citric acid and subcritical water. On the basis of Scenario CNC-2, CNC-3 changes the unit operations of acid hydrolysis and acid recovery. In Scenario CNC-3, citric acid
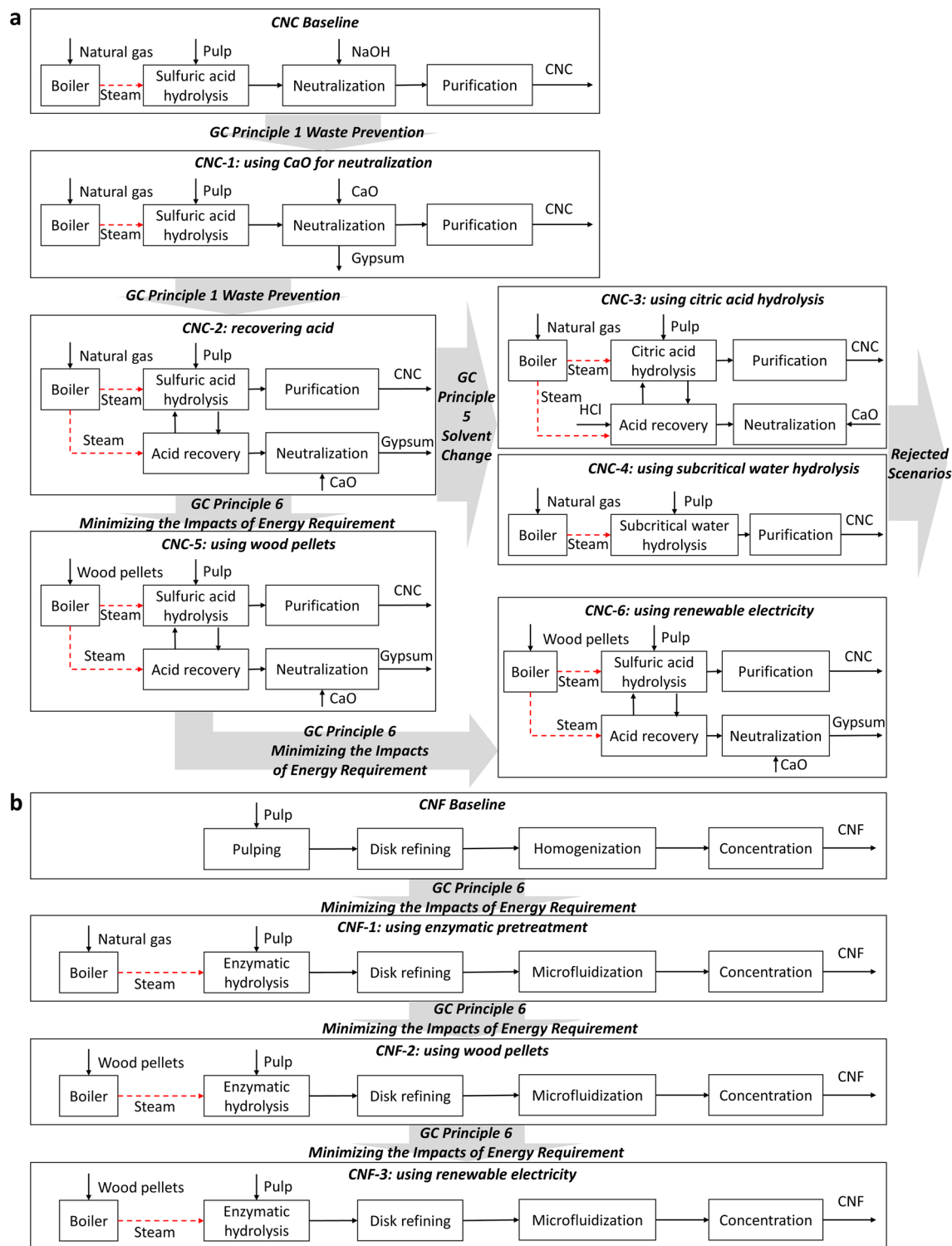
**Fig. 2** Derived improvement pathway and summarized process flowcharts. (a) CNC production. (b) CNF production. The final product of CNC and CNF is at 8% consistency. In (a), the CNC baseline employs sulfuric acid for hydrolysis and NaOH for neutralization without acid recovery. Following GC Principle 1 of waste prevention, Scenario CNC-1 replaces NaOH with CaO for neutralization that generates gypsum as a valuable byproduct. Based on Scenario CNC-1, Scenario CNC-2 further recovers sulfuric acid from the hydrolysate. Scenario CNC-3 and Scenario CNC-4 use citric acid and subcritical water as the hydrolysis solvent, respectively, following the GC Principle 5 of solvent change. Scenario CNC-5 and CNC-6 explore alternative fuel (residue-derived wood pellets) and electricity source (wind power), respectively, by following Principle 6 minimizing impacts of energy requirements. In (b), the CNF baseline deploys mechanical treatment as a common method. To potentially reduce the high energy consumption of the CNF baseline, Scenario CNF-1 adds enzymatic hydrolysis as pretreatment to reduce the polymer length, following GC Principle 6 minimizing the impacts of energy requirements. By applying the GC Principle 6, Scenario CNF-2 combusts wood pellets as renewable fuel; Scenario CNF-3 adopts renewable electricity rather than grid electricity.

hydrolysis is operated at 120 °C for 4.5 h with 60 wt% citric acid fed in and 7% pulp consistency.[39] After being separated from the hydrolysate in the centrifuges, the citric acid solution is recovered by ion exchange.[63] Other than using citric acid, Scenario CNC-4 employs subcritical water for hydrolysis that uses water as the hydrolyzing agent in a high-pressurized reactor.[50,64] The advantage of subcritical water hydrolysis is that it is free of substantial usage of acid; therefore, no need for recovery.

GC Principle 6 mentions that the economic and environmental impacts of the energy requirements should be minimized.[15] Rather than combusting natural gas for heat supply, Scenario CNC-5 utilizes the biomass solid fuel boiler by combusting wood pellets to provide the heat source.

Electricity is an important energy source in CNC production. Switching from current grid electricity (majorly generated by fossil fuel) to renewable electricity can reduce the GWP of CNC production. On the basis of Scenario CNC-5, Scenario CNC-6 further explores the impacts of using renewable electricity for the CNC plant by using onshore wind power.

### 2.4. Cellulose nanofibril production

In this study, the feedstock for CNF production is northern bleached softwood kraft (NBSK) pulp, a common type of pulp in the market.[46] NBSK pulp has been used as feedstock in the CNF pilot plant[65,66] and other studies.[46,67–69] The compositions of the dissolving pulp are 85% (*dry basis*) cellulose, 14% (*dry basis*) hemicellulose, and 1% lignin (*dry basis*), with 11% moisture content (*dry basis*).[46,70]

For CNF production, there are 4 scenarios as mentioned above (all the technical and modeling details are available in ESI Section S3†). The CNF baseline process uses mechanical treatment. The NBSK pulp and water are mixed in the hydropulper to achieve 3 wt% consistency and transferred to a buffer tank and re-circulated to a dual-disk disk refiner. Then, the stream passes through the homogenization at 1000 bar with one pass.[71] Finally, the CNF is concentrated by ultrafiltration to derive the final product. High energy consumption for producing CNF is a major disadvantage compared to CNC or cellulose microfibrils.[35] According to the GC Principle 6, increasing the overall process energy efficiency is important for minimizing the impacts of energy requirements.[15] To achieve this, pretreatment of the pulp can be one solution.[27] Hence, Scenario CNF-1 selected enzymatic hydrolysis as the pretreatment method to compare with the CNF baseline process. After the pulp shredder, the pulp is mixed with enzyme and buffer solution for enzymatic hydrolysis. After the enzymatic hydrolysis, the pulp is diluted to 1 wt% for disk refining and microfluidization. Similar to Scenario CNC-5 and CNC-6, Scenario CNF-2 utilizes wood pellets as the fuel source; Scenario CNF-3 further deploys wind power.

### 2.5. End-of-life of cellulose nanocrystals and cellulose nanofibrils

In this study, CNC and CNF are assumed to be landfilled with landfill gas recovery. Landfilled CNC or CNF majorly emits Greenhouse Gas (GHG) emissions (mainly $CO_2$ and $CH_4$) through the decay process.[72] Since CNC and CNF contain a neglectable amount of nutrient elements or other elements, this study only accounts for the GHG emissions from landfill gas. However, future research can include more emissions depending on the data availability. Due to the high GWP factor and energy value of $CH_4$, landfill gas recovery for energy generation is increasingly practiced in the U.S.[73] The GWP of CNC/CNF end of life were estimated by two steps: (1) the GHG emissions of landfill gas were evaluated by using the Intergovernmental Panel on Climate Change (IPCC) First Order Decay (FOD) method;[72] (2) it is assumed that part of the landfill gas is recovered, and then combusted for power generation. The details of landfill and landfill gas recovery are described in ESI Section S6 and Table S3.†

### 2.6. Life cycle assessment for cellulose nanomaterials

The cradle-to-grave LCAs were conducted in this study to assess the environmental performance of CNC and CNF production in the U.S., following ISO14040 and 14044 standards.[10,74] The cradle-to-grave system boundary includes raw material extraction, transportation, production, and end-of-life of CNC and CNF. Since cellulose nanomaterials have broad applications (*e.g.*, electronics, coating), this study does not include the use phase (*e.g.*, electronic usage). The use phase can be added in future research for specific CNC/CNF applications. Two functional units are used. A quantity of 1 dry kg of cellulose nanomaterials is the mass-based functional unit, which is widely used in the previous LCA literature of CNC and CNF.[35] The LCA results are then converted to the performance-based functional unit that incorporates material performance, specific tensile strength (see ESI Section S7 for details†).[75,76]

Different scenarios of CNC and CNF productions are developed to analyze the impacts of implementing GC principles. In each scenario, a process-based model was established to generate the mass and energy balance data that are utilized as life-cycle inventory (LCI) data in the LCA. The LCI of producing fuels, chemicals, and electricity (background processes) were collected from the ecoinvent 3.6 cut-off database[77] and are documented in ESI Table S4.†

The LCI data for producing NBSK pulp (for CNF production) was derived from the study by Thomas and Liu,[78] and shown in ESI Table S5.† The cradle-to-gate life-cycle environmental impacts of producing viscose grade dissolving pulp (for CNC production) were based on the work by Echeverria *et al.* and shown in ESI Table S6.†[58] The emission factors of combusting natural gas and wood pellet follow the U.S. Environmental Protection Agency (EPA) AP-42 External Combustion Sources emission factors for natural gas and wood residue combustion.[79] In this study, the feedstock pulp contains biogenic carbon that has two destinations. One is in nanocellulose that ends in landfill; the other is emitted as sugars or other organic compounds (*e.g.*, unreacted cellulose, furfural) to wastewater. The biogenic carbon ending in landfills is tracked by using the IPCC FOD method as mentioned above. In this study, the biogenic carbon in wastewater is

assumed to be eventually oxidized into $CO_2$ that is emitted to the atmosphere.

For the life cycle impact assessment method, as mentioned above, this study uses the GWP factors by the IPCC AR6 GWP-100 factors and TRACI 2.1 by U.S. EPA.[80,81] Hence, 10 impact categories are used: acidification, human health cancer, human health noncancer, ecotoxicity, eutrophication, fossil fuel depletion, global warming, ozone depletion, respiratory effects, and smog formation.

### 2.7. Techno-economic analysis for cellulose nanomaterials

The TEA investigates the CNC and CNF plant that produces 25–100 dry t cellulose nanomaterials per day. The capacity of 50 dry t per day is the plant scale used in the previous literature.[46,47] The selected indicator of economic performance is the minimum selling price (MSP). MSP was calculated by the discounted cash flow rate of return (DCFROR) analysis conducted in Microsoft Excel.[82] The MSP was derived by setting the 10% IRR and the Net Present Value (NPV) to be zero.[82] The year of analysis is 2020 given the data availability. The key assumptions of the TEA are shown in ESI Tables S7 and S8.† In TEA, the original purchased costs, installation factors, equipment scaling factors, material and energy prices, and feedstock costs were collected from the literature and discussed in ESI Section S8 and Tables S9–S12 for capital expenditures, and ESI Section S9 and Tables S13–S16 for operating expenditures.†

### 2.8. Eco-efficiency analysis

We adopt the indicator, ECE, proposed by Hellweg *et al.*[19] to quantify the eco-efficiency performance. $ECE_{A,B}$ is measured as the net environmental benefit of technology A over technology B divided by the additional financial cost of technology A over technology B, as shown in eqn (1).[19] Technology A is defined as the more environmentally benign technology. In eqn (1), $IP_A$ and $IP_B$ is the environmental impact of technology A and B, respectively; $NC_A$ and $NC_B$ is the net financial cost of technology A and B, respectively.[19] According to the definition, the numerator of eqn (1) is always positive. If $NC_A > NC_B$ (or say $ECE_{A,B}$ is positive), it means the trade-offs appear between environmental and economic aspects. The larger $ECE_{A,B}$ is, the higher eco-efficient the technology A is over technology B.[19] If $NC_A < NC_B$ (or say ECE is negative), it means that the co-benefit exists between environmental and economic aspects for technology A over B. The larger the absolute value of ECE is, the higher the co-benefit of technology A is over technology B when harvesting the same amount of cost benefit. In this study, GWP is selected as the environmental impact indicator and MSP is chosen as the financial cost indicator. Each scenario is compared with the baseline (technology B). Hence, if ECE > 0, the absolute value of ECE indicates how much GWP can be reduced when MSP is increased by US$1; if ECE < 0, the absolute value of ECE indicates how much GWP can be reduced when MSP is decreased by US$1.

$$ECE_{A,B} = \frac{(-IP_A) - (-IP_B)}{NC_A - NC_B} \quad (1)$$

### 2.9. Scenario analysis

The derived scenarios for the case study of cellulose nanomaterials are shown in ESI Table S17.† As mentioned above, there are 7 scenarios in CNC production and 4 scenarios in CNF production, including the baselines. As mentioned above, the detailed flowcharts of scenarios are available in ESI Fig. S1–S7.†

## 3. Results and discussion

### 3.1. Life-cycle environmental performance of cellulose nanomaterials

**3.1.1. Cellulose nanocrystal scenarios.** Fig. 3 shows the normalized life-cycle impact assessment results of 1 dry kg CNC produced (see source data in ESI Table S18, and Fig. S8† for the results of the performance-based functional unit). As expected, the baseline has the second-highest environmental burdens across all impact categories (Scenario CNC-3 has the highest environmental impact), which are attributed to high consumption of $H_2SO_4$ (hydrolysis chemicals in ESI Table S18†) and NaOH (other chemicals in ESI Table S18†). For example, in the CNC baseline, NaOH contributes to 64.8% of the total GWP (17.7 $kgCO_2e$ per kg dry CNC). Changing the neutralizing agent from NaOH to CaO in Scenario CNC-1 reduces the impacts across all categories by 29.3%–88.8% as shown in Fig. 3, mainly due to lower environmental burdens of the upstream production of CaO needed to neutralize the same amount of acid (see ESI Table S18†).

Given the high contribution of $H_2SO_4$ to environmental burdens, Scenario CNC-2 recovering acid decreases the environmental impacts by 8.9%–68.7% across all categories compared to Scenario CNC-1. GWP of Scenario CNC-2 decreases by 44.5% (6.5 $kgCO_2e$ in Scenario CNC-2 *versus* 11.7 $kgCO_2e$ in Scenario CNC-1, see ESI Table S18†). Though chemical usage decreases, the energy-related GWP of Scenario CNC-2 is 58.3% higher than CNC-1 due to natural gas consumption of the acid recovery process.

The results of Scenarios CNC-3 and CNC-4 demonstrate the importance of solvent selection. In Fig. 3, Scenario CNC-3 using critic acid has the highest GWP (22.8 $kgCO_2e$ per kg dry CNC, even higher than the baseline), mainly contributed by hydrolysis chemicals citric acid and HCl (65.6% of total GWP, see ESI Table S18†). Scenario CNC-3 also shows much higher environmental burdens than Scenario CNC-2 (56.3%–547.3% higher across all categories). Hence, using citric acid with the current recovery technologies presented in this study is not environmentally favorable and therefore this scenario is rejected. Instead of using citric acid, Scenario CNC-4 employs subcritical water hydrolysis and results in much lower environmental burdens than CNC-3. Compared to Scenario CNC-2 that does not change solvents, Scenario CNC-4 shows lower environmental impacts in most categories except GWP (6.8 $kgCO_2e$ per kg dry CNC, 5.2% higher than Scenario CNC-2), eutrophication, fossil fuel depletion, and respiratory (17.6%–40.5% higher than Scenario CNC-2). This is mainly
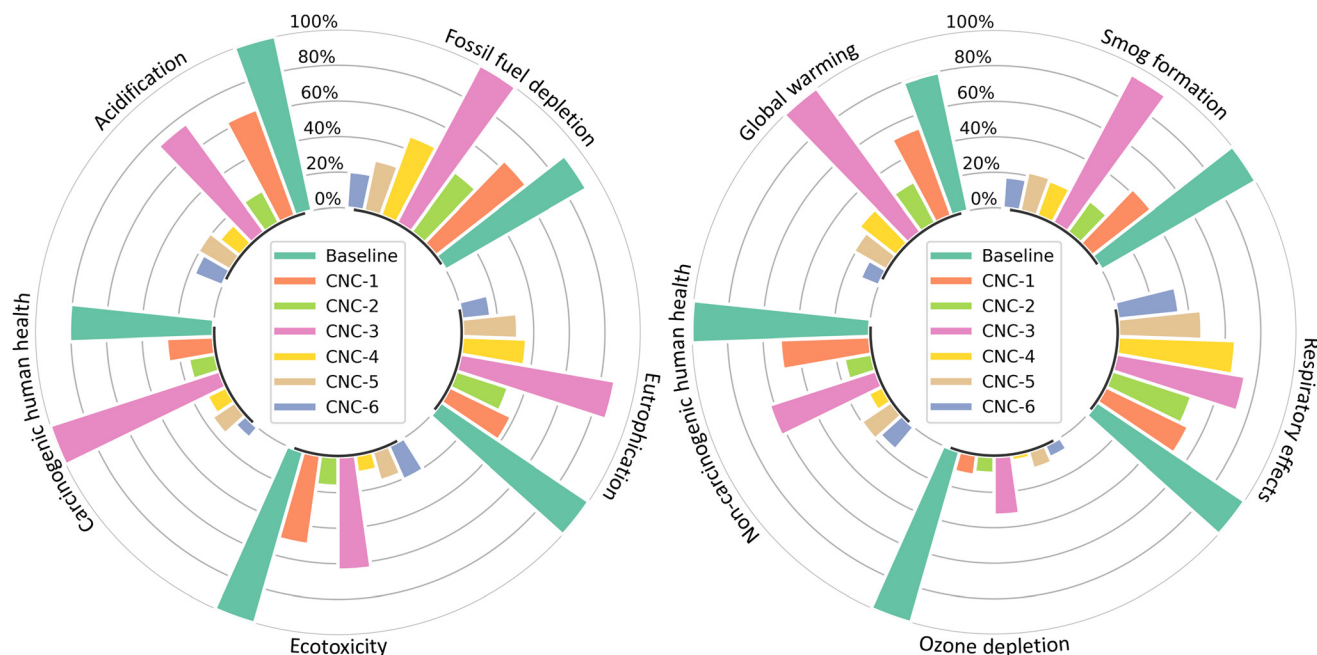
**Fig. 3** The normalized life-cycle environmental impacts of 1 dry kg CNC. CNC baseline: sulfuric acid for hydrolysis and NaOH for neutralization without acid recovery; Scenario CNC-1: sulfuric acid for hydrolysis and CaO for neutralization without acid recovery; Scenario CNC-2: sulfuric acid for hydrolysis and CaO for neutralization with acid recovery; Scenario CNC-3: citric acid for hydrolysis and CaO for neutralization with acid recovery; Scenario CNC-4: subcritical water for hydrolysis; Scenario CNC-5: combusting wood pellets, all other conditions same as Scenario CNC-2; Scenario CNC-6: wind power, all other conditions same as Scenario CNC-5.

because of the lower CNC yield (30%) of Scenario CNC-4 than Scenario CNC-2 (53.1%) (see ESI Table S18†). Hence, increasing CNC yield is recommended as the future research direction to improve the environmental performance of the subcritical water hydrolysis pathway.

The results of Scenarios CNC-5 and CNC-6 indicate the environmental trade-offs of energy decarbonization. Scenario CNC-5 combusts wood pellets instead of natural gas in Scenario CNC-2, resulting in 25.8% lower GWP and 40.3% lower fossil fuel depletion. However, Scenario CNC-5 has 0.3%–43.2% higher environmental burdens in other impact categories than Scenario CNC-2 due to higher non-greenhouse gas air emissions (*e.g.*, benzene, formaldehyde, fluorene) of wood pellet combustion. In Scenario CNC-6 which combusts wood pellets and further deploys wind power, GWP is finally reduced to 53.3% (2.6 kgCO$_2$e per kg dry CNC) of Scenario CNC-5 which uses grid electricity.

Overall, our results for CNC scenarios indicate larger environmental reduction potentials of chemical and waste related strategies than alternative energy supplies. The results of each scenario shed light on individual steps and combined pathways toward greener production of CNC materials. The sensitivity analysis of Scenario CNC-2 (see ESI Fig. S9, Table S19, and Section S10†) shows pulp consistency in acid hydrolysis and CNC conversion rate as the main impactors on GWP. Hence, increasing the pulp consistency in acid hydrolysis and the CNC conversion rate are recommended as future research priorities for reducing the carbon footprint of CNC. In previous literature, the cradle-to-gate (without end-of-life

stage) results range from 12.9 to 29.4 kgCO$_2$e per kg dry CNC.[38,43,45] The cradle-to-gate portion of our GWP result in the CNC baseline (17.5 kgCO$_2$e per kg dry CNC, see ESI Table S18†) is within the range of the previous literature.

The end-of-life stage (*i.e.*, landfill with landfill gas recovery for power generation) of CNC shows a minor influence on LCA results of the baseline, Scenarios CNC-1 and CNC-3. For example, in the CNC baseline, the end-of-life stage accounts for −3.6%–1.2% across all impact categories (negative values are the avoided environmental burdens of electricity substituted by landfill gas energy recovery) (see ESI Table S18†). The end-of-life impact increases to −28.3%–8.2% in Scenario CNC-6.

Integrating material performance into the LCA provides additional insights. Although the overall trends of the LCA results using the performance-based functional unit (see ESI Fig. S8†) are similar to the results based on 1 dry kg basis in Fig. 3, CNC-3 shows lower environmental impacts than the baseline due to better material performance, which is not the case using 1 kg dry CNC as the functional unit. However, CNC-3 is still rejected, given the higher environmental burdens than CNC-2 scenario.

**3.1.2. Cellulose nanofibrils scenarios.** Normalized life-cycle environmental impacts of CNF scenarios are shown in Fig. 4 (source data in ESI Table S20 and Fig. S10 for the results of the performance-based functional unit†). The CNF baseline shows the highest impacts across most impact categories except for ecotoxicity. For the CNF baseline, energy accounts for 57.7%–104.5% of all environmental impacts; feedstock contributes
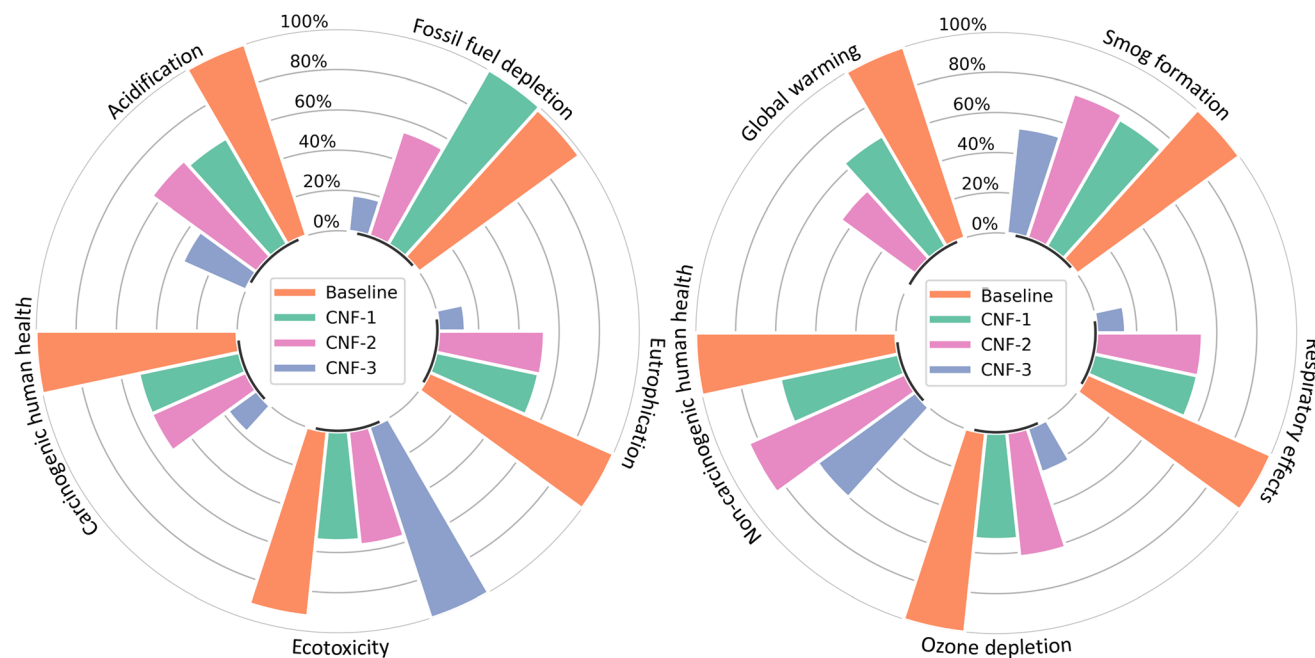
**Fig. 4** The normalized life-cycle environmental impacts of 1 dry kg CNF. CNF baseline: mechanical treatment; Scenario CNF-1: enzymatic hydrolysis as the pretreatment; Scenario CNF-2: combusting wood pellets, other settings are the same as Scenario CNF-1; Scenario CNF-3: wind power, other settings are the same with Scenario CNF-2. Note that the normalized result of Scenario CNF-3 GWP is 1.5% which is too small to be observed in the figure.

the second largest part by 10.7%–46.0% (see ESI Table S20†). CNF baseline has a lower life-cycle GWP (7.8 kgCO$_2$e per kg dry CNF) than CNC, because many chemicals intensively used in CNC production are not used in CNF production. Scenario CNF-1 deploys enzymatic hydrolysis to break the cellulose chain and reduce electricity consumption. Compared to the CNF baseline, the results of Scenario CNF-1 decrease by 26.9%–48.8% across all impact categories, except for fossil fuel depletion (a minor increase of 1.6% due to increased natural gas consumption and CNF loss during the process). GWP of Scenario CNF-1 decreases by 36.3% to 4.9 kgCO$_2$e per kg dry CNF. In addition, alternative energy supply scenarios CNF-2 and 3 show environmental trade-offs similar to the results of Scenarios CNC-5 and 6.

The end-of-life stage in Scenario CNF-3 (wind power) accounts for −47.2% to −5.3% of the life-cycle environmental impacts across all the categories except global warming (negative values due to the electricity displacement by recovering landfill gas for power generation). For example, for all CNF scenarios, the GWP of end-of-life includes the greenhouse gas (GHG) emissions from landfills (0.75 kgCO$_2$e per kg dry CNF) and electricity displacement (−0.54 kgCO$_2$e per kg dry CNF), and results in 0.21 kgCO$_2$e per kg dry CNF (see ESI Table S20†). For other impact categories, the end-of-life stage shows negative values, indicating the environmental benefits of recovering landfill gas for electricity generation. Hence, emissions from the end-of-life and landfill gas recovery are not neglectable, especially for Scenarios CNF-2 (total GWP 3.6 kgCO$_2$e per kg dry CNF) and CNF-3 (total GWP 0.1 kgCO$_2$e

per kg dry CNF). The cradle-to-gate GWP results (without end-of-life) in the CNF baseline (7.57 kgCO$_2$e per kg dry CNF, see ESI Table S20†) and CNF-1 (4.74 kgCO$_2$e per kg dry CNF, see ESI Table S20†) are within the range of the cradle-to-gate GHG emissions reported by the previous literature (0.79–23.0 kgCO$_2$e per kg dry CNF).[35,49,83]

The sensitivity analysis of Scenario CNF-1 (see ESI Fig. S11 and Section S10†) shows that pulp consistency in enzymatic hydrolysis has the largest impact on GWP, as it determines the water consumption, heat for hydrolysis, and electricity in hydrolysis and purification. The landfill gas recovery rate in the end-of-life stage, electricity consumption, and electricity carbon intensity are other important factors of GWP results. The results of the performance-based functional unit (see ESI Fig. S10†) show similar trends to the results on the basis of 1 dry kg CNF.

### 3.2. Economic feasibility of cellulose nanomaterials

The MSP and operating cost of CNC and CNF scenarios on 1 dry metric ton (t) of product basis are shown in Fig. 5a and b. The MSP, capital investment, and operating cost of varied plant capacities are displayed in ESI Tables S9–S16 and S21.† In Fig. 5a and b, the GWP results from LCA are exhibited as green triangles. Fig. 5c shows the MSP and GWP of all scenarios. Fig. 5d shows the ECE results of the scenarios. The results of performance-based functional unit are available in ESI Fig. S12† that shows similar trends to Fig. 5.

**3.2.1. Economic feasibility of cellulose nanocrystals.** In Fig. 5a, the CNC baseline results in the highest MSP of US
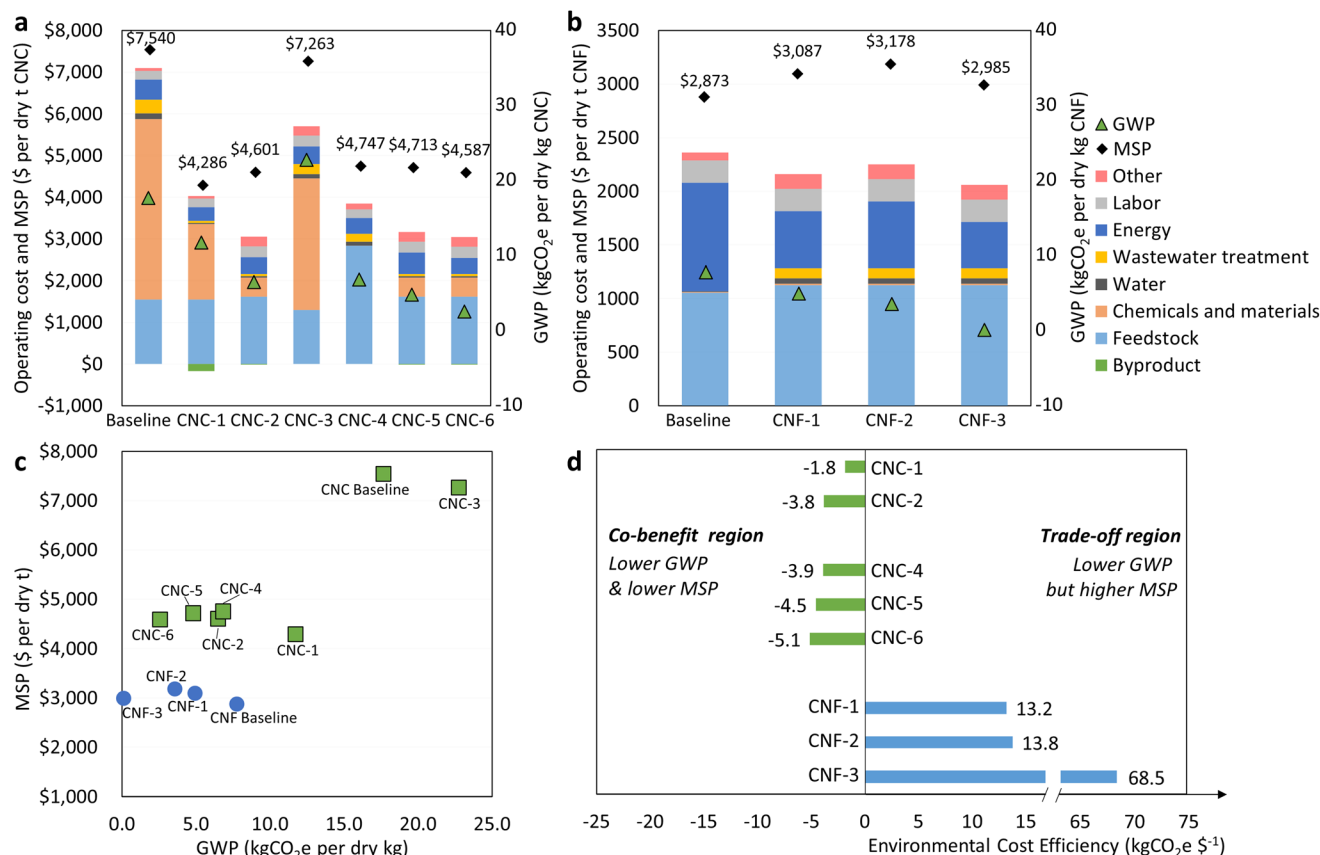
**Fig. 5** Minimum selling price, operating cost, global warming potentials, and eco-efficiency analysis results of scenarios at 50 dry t per day. (a) Cellulose nanocrystal scenarios. (b) Cellulose nanofibril scenarios. (c) Minimum selling price and GWP in all scenarios. (d) Environmental cost efficiency results of scenarios compared to the baseline. The minimum selling price (MSP) is displayed as diamonds (left vertical axis). GWP is displayed as triangles (right vertical axis). The plot of (c) is based on the MSP and GWP in (a) and (b). The results of environmental cost efficiency in (d) are derived based on GWP and MSP shown in (c). Positive values of environmental cost efficiency indicate the trade-off between environmental benefit and cost, and their absolute values show how much GWP can be reduced when MSP is increased by US$1. Negative values of environmental cost efficiency indicate the co-benefit of environmental benefit and cost, and their absolute values show how much GWP can be reduced when MSP is decreased by US$1. Note that the environmental cost efficiency of Scenario CNC-3 is not shown as Scenario CNC-3 has higher GWP than the CNC baseline.

$7540 per t dry CNC which are primarily contributed by chemicals and materials, specifically NaOH (US$3360 per t dry CNC) and $H_2SO_4$ (US$955 per t dry CNC, see ESI Tables S1 and S15†). Replacing the neutralizing agent NaOH by CaO in Scenario CNC-1 shows co-benefits of substantially reducing MSF (43.2% to US$4286 per t) and environmental impacts (GWP in Fig. 5 and other impacts in Fig. 3). Recovering acid in Scenario CNC-2 substantially reduces environmental burdens (Fig. 3) and cost of chemicals and materials (drops to US$461), but the overall MSP increases to US$4601, which is a trade-off. This is caused by much higher capital investment in Scenario CNC-2 (US$188.1 million) than Scenario CNC-1 (US$49.6 million, see ESI Table S9†). The high cost of citric acid (US$2682 per dry t CNC) makes Scenario CNC-3 economically unfavorable (MSP of US$7263 per t), similar to the LCA results. Scenario CNC-4 deploying subcritical water hydrolysis still shows slightly higher MSP (3.2%) than Scenario CNC-2. Scenario CNC-4 has lower capital investment (US$109.5 million), but this advantage is canceled out by lower

CNC yield than Scenario CNC-2. The results presented in Fig. 5a are consistent with previous economic analysis (US$4829–$10 974 per dry t CNC).[39,47]

The MSP of Scenario CNC-5 (combusting wood pellets) increases to US$4713 from US$4601 per t in Scenario CNC-2, though the GWP of Scenario CNC-5 decreases by 25.8% compared to Scenario CNC-2. When switching to wind power, the MSP of Scenario CNC-6 decreases to US$4587 per t. Note that the onshore wind power cost was estimated by the levelized cost of energy estimated by the U.S. National Renewable Energy Laboratory.[84] This can be further tailored depending on wind power type (e.g., onshore, fixed-bottom, floating offshore) and locations.[84] The sensitivity analysis of Scenario CNC-2 (see ESI Fig. S9 and Section S10†) exhibits pulp consistency in acid hydrolysis, internal rate of return (IRR), plant capacities, and CNC conversion rate as the main drivers of the MSP. For example, increasing the CNC conversion rate from 53.1% to 65.7% can reduce the MSP to US$4085 per dry t CNC.[60] Future research can further explore

the methods to increase CNC yield,[85] especially for large-scale production.

**3.2.2. Economic feasibility of cellulose nanofibrils.** Fig. 5b shows the MSP and operating cost of CNF scenarios at the capacity of 50 dry t per day. Across all CNF scenarios, feedstock cost is the largest contributor to the MSP, ranging from US$1055 in the CNF baseline to US$1128 in the other CNF scenarios. The difference is caused by cellulose degradation and loss in enzymatic hydrolysis and purification steps. The energy cost is the second largest contributor (US$429–$1011 per t dry CNF) due to energy-intensive mechanical treatment. The CNF baseline has an MSP of US$2873 per t in Fig. 5b. When enzymatic hydrolysis is employed as the pretreatment method, the MSP increases to US$3087 per t. This phenomenon has three contributors. The first one is the higher capital investment in Scenario CNF-1 (US$111.7 million, see ESI Table S10†) than US$60.5 million in the CNF baseline due to the added equipment for enzymatic hydrolysis. The second one is the higher feedstock cost due to cellulose degradation and yield loss as mentioned above. The third one is the largely decreased energy cost from US$1011 in the CNF baseline to US$530 in Scenario CNF-1. As an integrated effect of the three major causes, Scenario CNF-1 shows higher MSP than the baseline. However, Scenario CNF-1 has lower environmental impacts than the baseline (*e.g.*, 5.0 kgCO$_2$e in CNF-1 and 7.8 kgCO$_2$e in the baseline), which is a trade-off. By switching to wood pellets, the MSP is further increased to US$3178 per t due to higher energy cost per MJ than natural gas. Scenario CNF-3 shows the MSP of US$2985 per t by changing the grid electricity to wind power. The trends of Scenarios CNF-2 and CNF-3 in Fig. 5b are similar to Scenarios CNC-5 and CNC-6 in Fig. 5a. The sensitivity analysis of Scenario CNF-1 (see ESI Fig. S11 and Section S10†) shows that plant capacity, IRR, electricity cost, and pulp consistency in enzymatic hydrolysis, are the main drivers of the MSP. The MSP results in this study (US$2873–3178 per t dry CNF) are higher than the previous study de Assis *et al.*[46] (MSP US$1893–$2440 per t dry CNF), due to more unit operations deployed in this study to refine microfibrils to nanofibrils.

### 3.3. Eco-efficiency analysis

Fig. 5c co-presents MSP and GWP results of all scenarios; Fig. 5d shows the ECE results of CNC and CNF scenarios. ECE is calculated as the net environmental benefit of scenarios over baselines divided by the financial cost differences between scenarios and baselines. A positive ECE reflects a trade-off between higher costs and lower environmental burdens than the baseline. In other words, a positive ECE shows how much environmental burdens can be reduced by increasing the cost by US$1. A negative ECE, on the other hand, reflects a co-benefit of simultaneously reducing cost and environmental impacts, specifically showing how much environmental burdens can be reduced simultaneously with a cost reduction of US$1. Since CNC-3 is rejected given higher environmental burdens than CNC-2, CNC-3 is not included in ECE analysis according to the definition in Section 2.8. All CNF scenarios fall into trade-off regions. Scenario CNF-3 has higher ECE (68.5 kgCO$_2$e per $) than Scenarios CNF-1 (13.2 kgCO$_2$e per $) and Scenario CNF-2 (13.8 kgCO$_2$e per $). This is mainly contributed by wind power that largely reduces GWP and electricity cost. Wind power in Scenario CNF-3 results in a decrease of GWP by 7.7 kgCO$_2$e per kg dry CNF and an increase of MSP by US$111.8 per t dry CNF, compared to the CNF baseline. Scenario CNF-2 without wind power shows a much smaller GWP decrease (by 4.2 kgCO$_2$e per kg dry CNF) but a larger MSP increase (US$304.9 per t dry CNF). The MSP increase can be mitigated in the future by lowering the cost of renewable energy. In contrast to the CNF scenarios, CNC scenarios show co-benefits as shown in Fig. 5a. As the value of ECE shows the magnitude of environmental burden changes when 1 unit of financial performance is changed, the ECE results of different scenarios show the extent to which co-benefits or trade-offs exist for various process design choices, informing decision making towards maximum environmental cost-effectiveness. For example, CNF scenarios all have trade-offs, but Scenario CNF-3 has the highest ECE in Fig. 5d, indicating the largest environmental benefits when increasing the same US$1 cost. Thus, Scenario CNF-3 is the most favorable in terms of eco-efficiency. This conclusion is consistent with the results shown in Fig. 5b where three CNF scenarios all have higher MSP than the baseline, but Scenario CNF-3 has a lower GWP and MSP than Scenarios CNF-1 and 2.

For CNC scenarios, decision-makers can decide the best option depending on their targets of GWP reduction and budget or technological limits. However, ECE values provide additional information on the effectiveness of using their investment in reducing environmental burdens. When the cost benefits of various scenarios are similar, the higher absolute value of negative ECE is better. For example, Scenario CNC-5 shows better results (−4.5 kgCO$_2$e per $) than Scenario CNC-4 (−3.9 kgCO$_2$e per $) when MSP reduction compared to the baseline is similar (US$2793 for CNC-4 and US$2827 for CNC-5). These results demonstrate the usefulness of the framework and ECE indicator in supporting decision-making for sustainable cellulose material production. This case study only uses GWP and MSP for demonstration, but other indicators (*e.g.*, other environmental impacts presented in this study or aggregated environmental impacts as shown in the study by Van Schoubroeck *et al.*[86]) can be used, depending on decision-makers' needs and preferences. Moreover, ECE provides insights on trade-offs and co-benefits, but it should not be used alone without reporting the absolute values of environmental and economic performance which provides insights on the scale of financial investment and environmental issues, both of which are important for decision making.[19]

## 4. Conclusions

This study develops a modeling framework to support the decision-making for producing more sustainable materials. The framework is demonstrated by a case study of cellulose nanomaterials produced by various pathways in the U.S. The

pathways are identified based on the applicable GC principles. For CNC, the life-cycle GWP across scenarios is 2.6–17.7 kgCO$_2$e per kg dry CNC; the MSP is US\$4286–\$7540 per dry t CNC. Other environmental impacts such as acidification, eutrophication, and human health impacts, are also quantified. The results show that changing the neutralization agent from NaOH to CaO in CNC production largely reduces the life-cycle environmental impacts and MSP. The environmental impacts can be further reduced by adding acid recovery, although this change requires additional capital investment. Subcritical water is a better solvent than citric acid in terms of both environmental impacts and MSP. Future improvement in CNC yield can further reduce the GWP and MSP of the subcritical water pathway. For CNF, the life-cycle GWP across scenarios is 0.1–7.8 kgCO$_2$e per kg dry CNF; the MSP is US\$2873–\$3178 per dry t CNF. Enzymatic hydrolysis in pretreatment reduces the overall environmental impacts but increases MSP of CNF scenarios. In both CNC and CNF scenarios, renewable energy sources reduce most environmental impacts but not necessarily MSP. The eco-efficiency analysis assesses the trade-offs or co-benefits of economic and environmental performances of various scenarios and identifies the most cost-effective routes to reduce the environmental burdens, *i.e.*, using sulfuric acid with acid recovery and CaO neutralization combined with renewable fuel and electricity for CNC, and using enzymatic hydrolysis combined with renewable fuel and electricity for CNF. The case study demonstrates how LCA and TEA can be coupled with GC and eco-efficiency analysis in one consistent framework to identify more sustainable pathways of cellulose material production. This framework is broadly applicable and can be applied to other materials to support process design and optimization towards more sustainable directions.

## Author contributions

Y. Y. and K. L. designed the idea. Y. Y. supervised this study. K. L., H. S. W., T. L., C. A. A. collected and analyzed the data. K. L. built the process simulation models. K. L., H. S. W. and T. L. conducted the LCA, TEA, and sensitivity analysis. R. A. V. and Y. Z. provided suggestions for LCA and TEA. K. L. and H. S. W. visualized the results. K. L., H. S. W., T. L., C. A. A. wrote the draft. Y. Y., R. A. V., and Y. Z. revised the manuscript. All the authors contributed to writing and finalizing the manuscript.

## Conflicts of interest

The authors declare no conflicts of interest.

## Acknowledgements

## References

1 S. A. Mazari, E. Ali, R. Abro, F. S. A. Khan, I. Ahmed, M. Ahmed, S. Nizamuddin, T. H. Siddiqui, N. Hossain, N. M. Mubarak and A. Shah, *J. Environ. Chem. Eng.*, 2021, **9**, 105028.

2 L. M. Gilbertson, L. Pourzahedi, S. Laughton, X. Gao, J. B. Zimmerman, T. L. Theis, P. Westerhoff and G. V. Lowry, *Nat. Nanotechnol.*, 2020, **15**, 801–810.

3 M. M. Khin, A. S. Nair, V. J. Babu, R. Murugan and S. Ramakrishna, *Energy Environ. Sci.*, 2012, **5**, 8075–8109.

4 M. M. Falinski, D. L. Plata, S. S. Chopra, T. L. Theis, L. M. Gilbertson and J. B. Zimmerman, *Nat. Nanotechnol.*, 2018, **13**, 708–714.

5 M. F. Ashby, *Materials and the environment: eco-informed material choice*, Elsevier, 2012.

6 C. W. Babbitt and E. A. Moore, *Nat. Nanotechnol.*, 2018, **13**, 621–623.

7 S. Gavankar, S. Suh and A. F. Keller, *Int. J. Life Cycle Assess.*, 2012, **17**, 295–303.

8 C. A. de Assis, L. G. Greca, M. Ago, M. Y. Balakshin, H. Jameel, R. Gonzalez and O. J. Rojas, *ACS Sustainable Chem. Eng.*, 2018, **6**, 11853–11868.

9 A. Ahmed, I. Hassan, T. Ibn-Mohammed, H. Mostafa, I. M. Reaney, L. S. C. Koh, J. Zu and Z. L. Wang, *Energy Environ. Sci.*, 2017, **10**, 653–671.

10 ISO, *ISO 14044: Environmental Management, Life Cycle Assessment, Requirements and Guidelines*, 2006.

11 K. Lan, B. Zhang and Y. Yao, *One Earth*, 2022, 1–14.

12 T. Terlouw, C. Bauer, L. Rosa and M. Mazzotti, *Energy Environ. Sci.*, 2021, **14**, 1701–1721.

13 M. Metzger, M. M. Besli, S. Kuppan, S. Hellstrom, S. Kim, E. Sebti, C. V. Subban and J. Christensen, *Energy Environ. Sci.*, 2020, **13**, 1544–1560.

14 N. R. Baral, O. Kavvada, D. Mendez-Perez, A. Mukhopadhyay, T. S. Lee, B. A. Simmons and C. D. Scown, *Energy Environ. Sci.*, 2019, **12**, 807–824.

15 P. Anastas and N. Eghbali, *Chem. Soc. Rev.*, 2010, **39**, 301–312.

16 E. S. Beach, Z. Cui and P. T. Anastas, *Energy Environ. Sci.*, 2009, **2**, 1038–1049.

17 L. M. Gilbertson, J. B. Zimmerman, D. L. Plata, J. E. Hutchison and P. T. Anastas, *Chem. Soc. Rev.*, 2015, **44**, 5758–5777.

18 J. B. Zimmerman, P. T. Anastas, H. C. Erythropel and W. Leitner, *Science*, 2020, **367**, 397–400.

19 S. Hellweg, G. Doka, G. Finnveden and K. Hungerbühler, *J. Ind. Ecol.*, 2005, **9**, 189–203.

20 G. Huppes and M. Ishikawa, *J. Ind. Ecol.*, 2005, **9**, 43–46.

21 L. Zhang, X. Jia, Y. Ai, R. Huang, W. Qi, Z. He, J. J. Klemeš and R. Su, *J. Cleaner Prod.*, 2022, **345**, 131073.

22 O. Nechyporchuk, M. N. Belgacem and J. Bras, *Ind. Crops Prod.*, 2016, **93**, 2–25.

23 X. Xu, F. Liu, L. Jiang, J. Y. Zhu, D. Haagenson and D. P. Wiesenborn, *ACS Appl. Mater. Interfaces*, 2013, **5**, 2999–3009.

24 Y. Habibi, L. A. Lucia and O. J. Rojas, *Chem. Rev.*, 2010, **110**, 3479–3500.

25 A. B. Reising, R. J. Moon and J. P. Youngblood, *J. Sci. Technol. For. Prod. Processes*, 2012, **2**, 32–41.

26 Y. Cen, Z. Xiang, T. Han, Y. Long and T. Song, *Cellulose*, 2022, **29**, 7193–7209.

27 Y. Qing, R. Sabo, J. Y. Zhu, U. Agarwal, Z. Cai and Y. Wu, *Carbohydr. Polym.*, 2013, **97**, 226–234.

28 L. Kong, D. Xu, Z. He, F. Wang, S. Gui, J. Fan, X. Pan, X. Dai, X. Dong, B. Liu and Y. Li, *Molecules*, 2019, **24**, 1–13.

29 W. Wang and S. Fu, *Cellulose*, 2020, **27**, 1009–1020.

30 S. Jacob, R. Reshmy, S. Antony, A. Madhavan, R. Sindhu, M. K. Awasthi, M. Kuddus, S. Pillai, S. Varjani, A. Pandey and P. Binod, *Bioengineered*, 2022, **13**, 12823–12833.

31 K. S. Ooi, S. Haszman, Y. N. Wong, E. Soidin, N. Hesham, M. A. A. Mior, Y. Tabata, I. Ahmad, M. B. Fauzi and M. H. M. Yunus, *Materials*, 2020, **13**, 1–17.

32 R. Sabo, A. Yermakov, C. T. Law and R. Elhajjar, *J. Renewable Mater.*, 2016, **4**, 297–312.

33 S. Zhu, H. Sun, Y. Lu, S. Wang, Y. Yue, X. Xu, C. Mei, H. Xiao, Q. Fu and J. Han, *ACS Appl. Mater. Interfaces*, 2021, **13**, 59142–59153.

34 H. Nadeem, M. Dehghani, G. Garnier and W. Batchelor, *J. Cleaner Prod.*, 2022, **342**, 130890.

35 R. Arvidsson, D. Nguyen and M. Svanström, *Environ. Sci. Technol.*, 2015, **49**, 6881–6890.

36 X. Z. Sun, D. Moon, T. Yagishita and T. Minowa, *Trans. ASABE*, 2013, **56**, 1061–1067.

37 S. Haroni, H. Z. Dizaji, H. Bahrami and M. G. Alriols, *Ind. Crops Prod.*, 2021, **173**, 114084.

38 H. Gu, R. Reiner, R. Bergman and A. Rudie, in Proceedings from the LCA XV Conference, 2015, pp. 33–42.

39 T. J. Bondancia, G. Batista, J. de Aguiar, M. V. Lorevice, A. J. G. Cruz, J. M. Marconcini, L. H. C. Mattoso and C. S. Farinas, *ACS Sustainable Chem. Eng.*, 2022, **10**, 4660–4676.

40 D. M. do Nascimento, A. F. Dias, C. P. de Araújo Junior, M. de F. Rosa, J. P. S. Morais and M. C. B. de Figueirêdo, *Ind. Crops Prod.*, 2016, **93**, 58–65.

41 R. M. Leão, P. C. Miléo, J. M. L. L. Maia and S. M. Luz, *Carbohydr. Polym.*, 2017, **175**, 518–529.

42 P. Gallo Stampino, L. Riva, C. Punta, G. Elegir, D. Bussini and G. Dotelli, *Molecules*, 2021, **26**, 1–20.

43 K. C. Teh, R. R. Tan, K. B. Aviso, M. A. B. Promentilla and J. Tan, *Food Bioprod. Process.*, 2019, **118**, 13–31.

44 M. C. B. de Figueirêdo, M. de Freitas Rosa, C. M. L. Ugaya, M. D. S. M. de Souza Filho, A. C. C. da Silva Braid and L. F. L. de Melo, *J. Cleaner Prod.*, 2012, **35**, 130–139.

45 S. Zargar, J. Jiang, F. Jiang and Q. Tu, *Biofuels, Bioprod. Biorefin.*, 2022, **16**, 68–80.

46 C. A. de Assis, M. C. Iglesias, M. Bilodeau, D. Johnson, R. Phillips, M. S. Peresin, E. M. Bilek, O. J. Rojas, R. Venditti and R. Gonzalez, *Biofuels, Bioprod. Biorefin.*, 2017, **12**, 251–264.

47 C. A. de Assis, C. Houtman, R. Phillips, E. M. Bilek, O. J. Rojas, L. Pal, M. S. Peresin, H. Jameel and R. Gonzalez, *Biofuels, Bioprod. Biorefin.*, 2017, **11**, 682–700.

48 M. Jonoobi, A. P. Mathew and K. Oksman, *Ind. Crops Prod.*, 2012, **40**, 232–238.

49 D. Moon, M. Sagisaka, K. Tahara and K. Tsukahara, *Sustainablility*, 2017, **9**, 2368.

50 L. P. Novo, J. Bras, A. García, N. Belgacem and A. A. S. Curvelo, *ACS Sustainable Chem. Eng.*, 2015, **3**, 2839–2846.

51 N. U. M. Nizam, M. M. Hanafiah and K. S. Woon, *Nanomaterials*, 2021, **11**, 1–27.

52 J. Kirchherr, D. Reike and M. Hekkert, *Resour., Conserv. Recycl.*, 2017, **127**, 221–232.

53 G. Moraga, S. Huysveld, F. Mathieux, G. A. Blengini, L. Alaerts, K. Van Acker, S. de Meester and J. Dewulf, *Resour., Conserv. Recycl.*, 2019, **146**, 452–461.

54 A. G. Parvatker and M. J. Eckelman, *ACS Sustainable Chem. Eng.*, 2019, **7**, 350–367.

55 A. W. Zimmermann, J. Wunderlich, L. Müller, G. A. Buchner, A. Marxen, S. Michailos, K. Armstrong, H. Naims, S. McCord, P. Styring, V. Sick and R. Schomäcker, *Front. Energy Res.*, 2020, **8**, 1–23.

56 W. Wang, S. Fu, S. Y. Leu and C. Dong, *Cellulose*, 2018, **25**, 6465–6478.

57 Z. Zhu, W. Wang, X. Wang, X. Zhao, N. Xia, F. Kong and S. Wang, *Cellulose*, 2021, **28**, 9661–9676.

58 D. Echeverria, R. Venditti, H. Jameel and Y. Yao, *Environ. Sci. Technol.*, 2022, **56**, 4578–4586.

59 H. Sixta, *Handbook of Pulp*, Wiley-VCH Verlag GmbH & Co. KGaA, Weinheim, Germany, 2006.

60 Q. Wang, X. Zhao and J. Y. Zhu, *Ind. Eng. Chem. Res.*, 2014, **53**, 11007–11014.

61 J. Lemaire, C. L. Blanc, F. Duval, M. A. Théoleyre and D. Pareau, *Sep. Purif. Technol.*, 2016, **166**, 181–186.

62 F. J. Wolfaardt, L. G. L. Fernandes, S. K. C. Oliveira, X. Duret, J. F. Görgens and J. M. Lavoie, *Energy Convers. Manage.: X*, 2021, **10**, 100074.

63 J. Wang, Z. Cui, Y. Li, L. Cao and Z. Lu, *J. Cleaner Prod.*, 2020, **249**, 119315.

64 L. P. Novo, J. Bras, A. García, N. Belgacem and A. A. da S. Curvelo, *Ind. Crops Prod.*, 2016, **93**, 88–95.

65 D. A. Johnson, in TAPPI Nanotechnology Conference, Vancouver, CA, 2014.

66 The University of Maine, UMaine Nanomaterial Pilot Plant, **https://umaine.edu/pdc/nanocellulose/umaine-nanomaterial-pilot-plant/**.

67 X. Tian, P. Lu, X. Song, S. Nie, Y. Liu, M. Liu and Z. Wang, *Cellulose*, 2017, **24**, 3929–3942.

68 Y. Wen, Z. Yuan, J. Qu, C. Wang and A. Wang, *ACS Sustainable Chem. Eng.*, 2020, **8**, 2688–2697.

69 N. Saba, F. Mohammad, M. Pervaiz, M. Jawaid, O. Y. Alothman and M. Sain, *Int. J. Biol. Macromol.*, 2017, **97**, 190–200.

70 A. K. Timo and L. V. Luukkainen, *Cellulose*, 2020, **27**, 6961–6976.

71 S. Ang, V. Haritos and W. Batchelor, *Cellulose*, 2019, **26**, 4767–4786.

72 S. Towprayoon, T. Ishigaki, C. Chiemchaisri, A. O. Abdel-Aziz, M. E. Hunstone, C. Jarusutthirak, M. Ritzkowski and M. Thomsen, in *2019 Refinement to the 2006 IPCC Guidelines for National Greenhouse Gas Inventories*, 2019, vol. 5, pp. 6.1–6.49.

73 US EPA, Landfill Methane Outreach Program (LMOP), **https://www.epa.gov/lmop/project-and-landfill-data-state**.

74 ISO, *ISO 14040:2006 Environmental management—Life cycle assessment—Principles and framework*, 2006.

75 Q. Xia, C. Chen, Y. Yao, J. Li, S. He, Y. Zhou, T. Li, X. Pan, Y. Yao and L. Hu, *Nat. Sustainable*, 2021, **4**, 627–635.

76 S. Xiao, C. Chen, Q. Xia, Y. Liu, Y. Yao, Q. Chen, M. Hartsfield, A. Brozena, K. Tu, S. J. Eichhorn, Y. Yao, J. Li, W. Gan, S. Q. Shi, V. W. Yang, M. Lo Ricco, J. Y. Zhu, I. Burgert, A. Luo, T. Li and L. Hu, *Science*, 2021, **374**, 465–471.

77 G. Wernet, C. Bauer, B. Steubing, J. Reinhard, E. Moreno-Ruiz and B. Weidema, *Int. J. Life Cycle Assess.*, 2016, **21**, 1218–1230.

78 V. M. Thomas and W. Liu, *Assessment of Alternative Fibers for Pulp Production*, 2013.

79 US Environmental Protection Agency, *AP 42, Fifth Edition Compilation of Air Pollutant Emissions Factors*, 2009.

80 IPCC, *Climate Change 2021: The Physical Science Basis AR 6 Work Group I*, 2022.

81 M. Ryberg, M. D. M. Vieira, M. Zgola, J. Bare and R. K. Rosenbaum, *Clean Technol. Environ. Policy*, 2014, **16**, 329–339.

82 K. Lan, L. Ou, S. Park, S. S. Kelley, B. C. English, T. E. Yu, J. Larson and Y. Yao, *Renewable Sustainable Energy Rev.*, 2021, 110881.

83 Q. Li, S. Mcginnis, C. Sydnor, A. Wong and S. Renneckar, *ACS Sustainable Chem. Eng.*, 2013, **1**, 919–928.

84 T. Stehly, P. Beiter and P. Duffy, *2019 Cost of Wind Energy Review*, Golden, CO, United States, 2020.

85 L. Chen, Q. Wang, K. Hirth, C. Baez, U. P. Agarwal and J. Y. Zhu, *Cellulose*, 2015, **22**, 1753–1762.

86 S. Van Schoubroeck, G. Thomassen, S. Van Passel, R. Malina, J. Springael, S. Lizin, R. A. Venditti, Y. Yao and M. Van Dael, *Green Chem.*, 2021, **23**, 1700–1715.